FPN4

EG&G INC.

TECHNICAL REPORT

NUMBER B-3307
EGG-1183-299
6 MAY 1966

DIFFUSION OF DAMPED SINE-WAVE MAGNETIC FIELDS INTO METALS

CONTRACT NO. 92-2404

PREPARED BY

JONATHAN Z. FARBER

Approved by Raymond C. O'Rourke
Associate Division Manager - Research
Systems Division
EG&G, Inc.
Boston, Massachusetts 02215

PREPARED FOR
THE SANDIA CORPORATION
LIVERMORE, CALIFORNIA

SYSTEMS DIVISION
EDGERTON, GERMESHAUSEN & GRIER, INC

EG&G INC.

This paper is concerned with the diffusion of a strong, time-varying magnetic field of the form $H = H_o e^{-at} \sin \omega t$ into an aluminum conducting region of finite extent. The rise in temperature imparted to the metal by the diffusion process is assumed small enough so that its conductivity can be considered constant. The solution of the diffusion equation with such an inhomogeneous, time-varying boundary condition is effected by Laplace transform methods. The resultant diffusion field is expressed in terms of complimentary error functions of complex argument. The magnitude of the diffusion field is, of course, a function of both time and penetration distance; it is also dependent on two additional parameters: the damping rate and the angular frequency of the surface field. The complete behavior of the diffusion field is ascertained by both evaluating and plotting the time-variation of the magnetic field diffusion as a function of each of the other three parameters; all other quantities in each case being held constant. It is found that the diffusion field, like the surface field, is also a damped oscillatory function in time. The frequency of oscillation of the diffusion field decreases with increasing penetration distance and, for a given depth of penetration, exhibits a strange dependence on the damping rate associated with the surface field. As is expected, the peak value of the diffusion field decreases with increasing penetration distance. The fraction of the surface field that diffuses to a given depth of penetration in a given time depends markedly on the ratio $\frac{\omega}{a}$. For a given frequency, the greater the damping rate, the greater the percentage of diffusion.

EG&G INC.

TABLES

TABLE

EG&G INC.

Page

ILLUSTRATIONS

FIGURE

EG&G INC.

Page

FIGURE

SECTION I
INTRODUCTION

Magnetic pressures associated with the damped sine-wave magnetic fields produced by discharging a capacitor bank and establishing a ringing LRC circuit, are often used to impulsively load thin-walled metallic structures. This same method is also employed in the magnetic forming of metal. When the appropriate metal wall thicknesses are comparable to the skin depths of the applied fields, one can no longer neglect the diffusion of magnetic flux lines through the metal. This paper makes use of error functions of complex argument, recently shown to be of great importance in problems of heat conduction, to solve the diffusion equation with inhomogeneous boundary conditions and determine the diffusion of such time-varying magnetic fields.

Consider a strong, time-varying magnetic field that is suddenly applied to the surface of an aluminum conducting medium. If the magnetic field intensity is not sufficient to produce an appreciable fractional change in the temperature of the aluminum, it is not unreasonable to regard the conductivity of the metal as a constant. The one-dimensional diffusion of the magnetic field into the conductor is adequately described by the two Maxwell equations of electrodynamics:

$$\frac{\partial H}{\partial x} = -j \tag{1}$$

and

$$\frac{\partial E}{\partial x} = -\mu \frac{\partial H}{\partial t} \tag{2}$$

together with the constitutive relation

$$j = \sigma E \tag{3}$$

where

- x denotes the distance inward from the surface of the conductor,
- H is the magnetic field intensity,
- E is the electric field intensity,
- j is the electric current density, and
- μ is the magnetic permeability of the metal;

all quantities are in rationalized MKS units.

For the case of constant conductivity, these three equations can be combined to obtain the following single, linear, partial differential equation:

$$\frac{\partial^2 H}{\partial x^2} = \mu\sigma \frac{\partial H}{\partial t} \quad , \tag{4}$$

which is easily recognized as the diffusion equation generally associated with problems concerning heat flow.

The boundary and initial conditions must still be specified. Since the magnetic field is applied suddenly at some given time, the initial condition is

$$H(x, 0) = 0 \quad . \tag{5}$$

As mentioned earlier, the problem is that of a time-varying field applied to the surface of the metal. Choosing the specific case of a damped sinusoid, the appropriate boundary condition is

$$H(0, t) = H_o(\omega, a)\, e^{-at} \sin \omega t \tag{6}$$

where a is the damping rate and ω the angular frequency; both quantities are in units of reciprocal seconds. The constant, H_o, is independent of x and t, but can be a function of either the frequency and/or the damping rate. For a conducting region of finite extent, the field at the outer boundary must be finite and, furthermore, the maximum value of the diffusion field at the outer boundary must be less than the corresponding value at the inner boundary, ($x = 0$). Thus, if the outer boundary is located at $x = d$,

$$H^{max}(d, t) \leq H^{max}(0, t) \quad .$$

The diffusion equation can be easily solved by using integral transform methods when the boundary condition is homogeneous; i. e.,

$H = H_o$.[1] If the electrical conductivity is temperature dependent, the electrodynamical equations listed above are then coupled to the equations of heat flow, and the resulting differential equations are non-linear. In Reference 2 a solution of the non-linear diffusion problem with homogeneous boundary conditions was accomplished. The system of non-linear partial differential equations was reduced to a system of non-linear ordinary differential equations in a single variable by means of the transformation

$$\zeta = \sqrt{\mu\sigma}\,\frac{x}{\sqrt{t}} \quad .$$

In the present case, the inhomogeneous boundary condition precludes the use of this technique.

Since the surface field exists only for some $t > o$, this suggests the use of the Laplace Integral Transform with respect to the time variable; i. e.,

$$F(x, s) = \int_o^\infty e^{-st} H(x, t)\, dt \quad . \qquad (7)$$

The Laplace transform of the diffusion equation, Equation (4), then becomes

$$\frac{\partial^2 F}{\partial x^2} = \mu\sigma s F \quad , \qquad (8)$$

since $H(x, 0) = 0$.

One must also transform the boundary condition:

$$F(0, s) = H_o \int_o^\infty e^{-at} \sin \omega t\, e^{-st}\, dt = \frac{H_o \omega}{(s+a)^2 + \omega^2} \quad . \qquad (9)$$

The transformed differential equation is easily solved to yield, as the only admissible solution,

$$F(x, s) = A(s) \exp\left(-\sqrt{\mu\sigma s}\, x\right) . \qquad (10)$$

One can show that the positive exponential solution leads to values of the diffusion field, which violate the boundary condition at x = d.

The value of A(s) is easily obtained from Equation (9), and the complete solution in transform (frequency) space is

$$F(x, s) = \frac{H_o \omega}{(s+a)^2 + \omega^2} \exp\left(-\sqrt{\mu\sigma s}\, x\right) . \qquad (11)$$

The solution in real (x, t) space is then obtained by inverting the transform given by Equation (11). Thus,

$$H(x, t) = \frac{1}{2i} \frac{H_o}{2\pi i} \left[\int_{C-i\infty}^{C+i\infty} ds \, \frac{\exp\left(-\sqrt{\mu\sigma s}\, x\right)}{s + a - i\omega} e^{st} - \int_{C-i\infty}^{C+i\infty} ds \, \frac{\exp\left(-\sqrt{\mu\sigma s}\, x\right)}{s + a + i\omega} e^{st} \right] . \qquad (12)$$

Consider

$$I_1 = \frac{1}{2\pi i} \int_{C-i\infty}^{C+i\infty} \frac{ds \exp\left(-\sqrt{\mu\sigma s}\, x\right)}{s + a - i\omega} e^{st} . \qquad (13)$$

Multiplying both sides of this equation by $e^{(a-i\omega)t}$ and then differentiating under the integral sign, one obtains

$$\frac{\partial}{\partial t} I_1 e^{(a-i\omega)t} = e^{(a-i\omega)t} \frac{1}{2\pi i} \int_{C-i\infty}^{C+i\infty} ds \exp\left(-\sqrt{\mu\sigma s}\, x\right) e^{st} ds \,. \tag{14}$$

However, this integral is a well-known inverse transform and one finds that[3, 4]

$$\frac{\partial}{\partial t} I_1 e^{(a-i\omega)t} = e^{(a-i\omega)t} \frac{x}{2} \sqrt{\frac{\mu\sigma}{\pi t^3}} \exp\left(-\frac{x^2\mu\sigma}{4t}\right) . \tag{15}$$

Solving this differential equation for I_1,

$$I_1 = e^{-(a-i\omega)t} \frac{x}{2} \sqrt{\frac{\mu\sigma}{\pi}} \int_0^t \frac{e^{(a-i\omega)t'} \exp\left(\frac{-x^2\mu\sigma}{4t'}\right)}{t'^{3/2}} dt' . \tag{16}$$

Making the substitution $t' = \frac{1}{y^2}$,

$$I_1 = e^{-(a-i\omega)t} x\sqrt{\frac{\mu\sigma}{\pi}} \int_{t^{-\frac{1}{2}}}^{\infty} \exp\left(\frac{-x^2\mu\sigma\, y^2}{4} + \frac{b^2}{y^2}\right) dy \tag{17}$$

where $b^2 = a-i\omega$ is a complex number.

The solutions to this form of integral are error functions of complex argument. One finds that[5]

$$\int_{t^{-\frac{1}{2}}}^{\infty} \exp\left(-a^2y^2 + \frac{b^2}{y^2}\right) dy = \frac{\sqrt{\pi}}{4a} \exp\left(\frac{-a^2}{t} + b^2t\right) \left[w\left(b\sqrt{t} + i\frac{a}{\sqrt{t}}\right) + w\left(-b\sqrt{t} + i\frac{a}{\sqrt{t}}\right)\right] \tag{18}$$

where $w(x + iy)$ is the complementary error function of complex argument and is defined as

$$w(z) = e^{-z^2}\left(1 + \frac{2i}{\sqrt{\pi}}\int_0^z e^{t^2}\,dt\right) . \qquad (19)$$

This function, which has recently been shown to be of prime importance in problems involving heat conduction, was first tabulated with some degree of accuracy by Faddeeva and Terentev in 1954.[4] This function is discussed in some detail in Reference 5.

Making use of Equation (18), the expression for I_1 is rewritten as

$$I_1 = \frac{1}{2}\exp\left(\frac{-x^2\mu\sigma}{4t}\right)\left[w\left[-A\sqrt{t} + i\left(\frac{x}{2}\sqrt{\frac{\mu\sigma}{t}} + B\sqrt{t}\right)\right] + w\left[A\sqrt{t} + i\left(\frac{x}{2}\sqrt{\frac{\mu\sigma}{t}} - B\sqrt{t}\right)\right]\right] \qquad (20)$$

where A and B are the real and imaginary parts of $b = \sqrt{a - i\omega}$, respectively, and are as follows:

$$A = \left(\frac{\sqrt{a^2 + \omega^2} + a}{2}\right)^{1/2} \qquad (21)$$

and

$$B = \left(\frac{\sqrt{a^2 + \omega^2} - a}{2}\right)^{1/2} . \qquad (22)$$

In an analogous manner, the second integral in Equation (12) can be evaluated as

$$I_2 = \frac{1}{2\pi i}\int_{C-i\infty}^{C+i\infty} ds\,\frac{\exp\left(-\sqrt{\mu\sigma s}\,x\right)}{s + a + i\omega}\,e^{st} =$$

$$\frac{1}{2}\exp\left(\frac{-x^2\mu\sigma}{4t}\right)\left[w\left[A\sqrt{t}+i\left(\frac{x}{2}\sqrt{\frac{\mu\sigma}{t}}+B\sqrt{t}\right)\right]+w\left[-A\sqrt{t}+i\left(\frac{x}{2}\sqrt{\frac{\mu\sigma}{t}}-B\sqrt{t}\right)\right]\right] \tag{23}$$

Combining the results of Equations (20) and (23) with Equation (12), one obtains

$$H(x,t) = \frac{H_o}{4i}e^{-\zeta^2}\left[w[-\xi+i(\zeta+\eta)]+w[\xi+i(\zeta-\eta)]\right.$$

$$\left.-w[\xi+i(\zeta+\eta)]+w[-\xi+i(\zeta-\eta)]\right] \tag{24}$$

where

$$\xi = A\sqrt{t},$$

$$\eta = B\sqrt{t}, \text{ and}$$

$$\zeta = \frac{x}{2}\sqrt{\frac{\mu\sigma}{t}} \quad . \tag{25}$$

By making use of the several symmetry relations involving the error function of complex argument, the above solution is greatly simplified, and it will be conclusively demonstrated that this result is indeed real, rather than complex. One can show from Equation (19) and from the integral representation,

$$w(z) = \frac{i}{\pi}\int_{-\infty}^{\infty}\frac{e^{-t^2}\,dt}{z-t} \quad , \tag{26}$$

that the following symmetry relations are true:[5]

$$w(-x+iy) = \overline{w(x+iy)} \tag{27}$$

$$w(x-iy) = 2e^{y^2-x^2}(\cos 2xy + i\sin 2xy) - \overline{w(x+iy)} \tag{28}$$

$$w(-x-iy) = 2e^{y^2-x^2}(\cos 2xy - i \sin 2xy) - w(x + iy) \quad . \tag{29}$$

Making use of these relationships, the diffusion field solution can be displayed by either of the following forms.

For $\zeta \geq \eta$,

$$H(x, t) = \frac{H_o}{2} e^{-\zeta^2} \left[\text{Im } w[\xi + i(\zeta - \eta)] - \text{Im } w[\xi + i(\zeta + \eta)] \right] \quad . \tag{30}$$

For $\zeta < \eta$,

$$H(x, t) = \frac{H_o}{2} e^{-\zeta^2} \left[2 \exp - [\xi^2 - (\eta - \zeta)^2] \sin 2\xi(\eta - \zeta) + \text{Im } w[\xi + i(\eta - \zeta)] \right.$$

$$\left. - \text{Im } w[\xi + i(\eta + \zeta)] \right] \quad . \tag{31}$$

From this last result, one can readily see that the solution satisfies both the initial condition and the boundary condition at $x = 0$. When $t = 0$, ζ becomes infinite, $e^{-\zeta^2}$ approaches zero, and $H(x, 0) = 0$. When $x = 0$, $\zeta = 0$; and from Equation (31) one obtains the following:

$$H(0, t) = H_o e^{-(\xi^2 - \eta^2)} \sin 2\xi\eta \quad . \tag{32}$$

However, from the definitions of ξ, η, A, and B

$$\xi^2 - \eta^2 = (A^2 - B^2)t = at$$

$$\xi\eta = ABt = \frac{\omega t}{2}$$

and hence

$$H(0, t) = H_o e^{-at} \sin \omega t \tag{33}$$

which satisfies the boundary condition.

The diffusion field H(x, t) is a function of four variables: time, penetration distance, damping rate, and angular frequency. Some insight is gained into the nature of the diffusion field by evaluating H(x, t) as a function of time for different constant values of x, the other two variables, a and ω, being maintained fixed throughout. Values of H/H_o are listed in Table 1 for constant values of $a = 5.4 \times 10^4$ sec^{-1} and $\omega = 3.05 \times 10^5$ sec^{-1}, and these values are plotted in Figure 1. The values of x were chosen as the most interesting cases because they are comparable to the skin depth in aluminum at the aforementioned frequency. As can be seen from the plots in Figure 1, the field, at any given depth in the metal, varies as a damped oscillatory function of time. The period of oscillation increases with increasing penetration depth. The surface field, $H(x = 0) = H_s$, rises to its peak value after 4.4 microseconds, while the rise time to peak is accordingly 7.0 microseconds at $x = 3.048 \times 10^{-4}$ meter, 7.7 microseconds at $x = 4.064 \times 10^{-4}$ meter, and 8.5 microseconds at x = 5.080 meter. Similarly, the peak value of the diffusion field decreases with increasing penetration depth, as is expected.

The variation of half-period of oscillation of the diffusion field is depicted as a function of penetration depth in Figure 2. For given values of $a = 5 \times 10^4$ sec^{-1} and $\omega = 3.5 \times 10^5$ sec^{-1}, the half-period at a depth of 3.048×10^{-4} meter is observed to be 11.9 microseconds, compared to a half-period of 13.0 microseconds at a depth of 4.064×10^{-4} meter.

These times are considerably greater than the 9-microsecond half-cycle of the field at the surface.

For the case of a constant magnetic field applied to the surface of a conductor, the fields that diffuse into the metal never reach magnitudes

TABLE 1. TIME VARIATION OF H/H_o AS A FUNCTION OF PENETRATION DISTANCE FOR CONSTANT $a = 5.4 \times 10^4$ sec^{-1} AND FOR CONSTANT $\omega = 3.05 \times 10^5$ sec^{-1}

x	Time, Microseconds									
	1	2	3	4	5	6	7	8	9	10
0.000	0.284	0.513	0.675	0.757	0.763	0.699	0.580	0.418	0.238	0.053
2.540×10^{-4}	0.031	0.122	0.225	0.327	0.390	0.427	0.438	0.402	0.348	0.258
3.048×10^{-4}	0.015	0.091	0.177	0.262	0.335	0.375	0.394	0.376	0.338	0.276
3.556×10^{-4}	0.012	0.060	0.131	0.212	0.277	0.327	0.350	0.346	0.323	0.276
4.064×10^{-4}	0.007	0.040	0.112	0.169	0.232	0.286	0.310	0.315	0.303	0.269
4.572×10^{-4}	0.005	0.027	0.074	0.134	0.188	0.240	0.272	0.284	0.281	0.259
5.080×10^{-4}	0.003	0.018	0.055	0.102	0.153	0.195	0.237	0.252	0.257	0.244

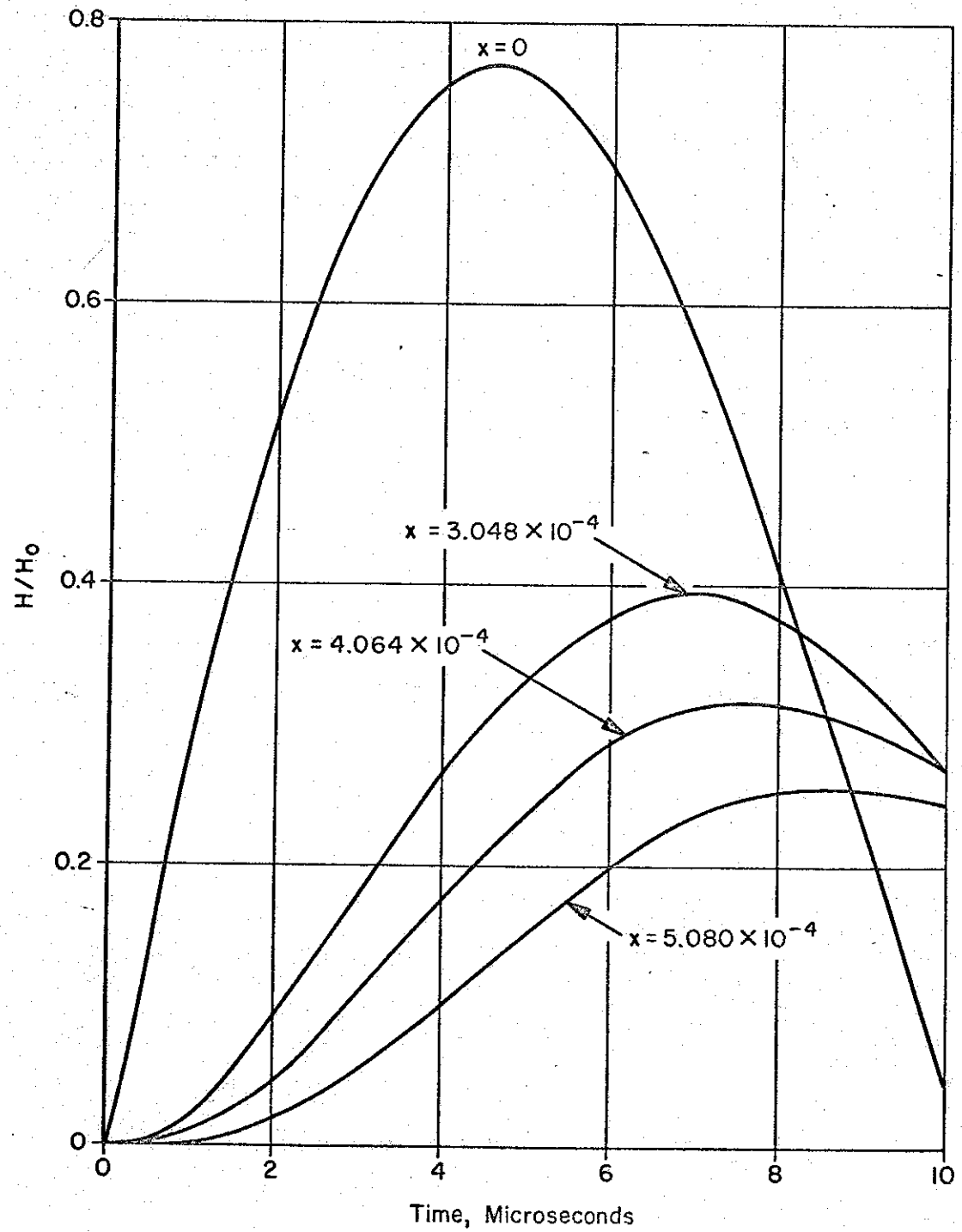

Figure 1. Time variation of diffusion field as a function of penetration distance for constant $a = 5.4 \times 10^{4}$ sec^{-1} and for constant $\omega = 3.05 \times 10^{5}$ sec^{-1}.

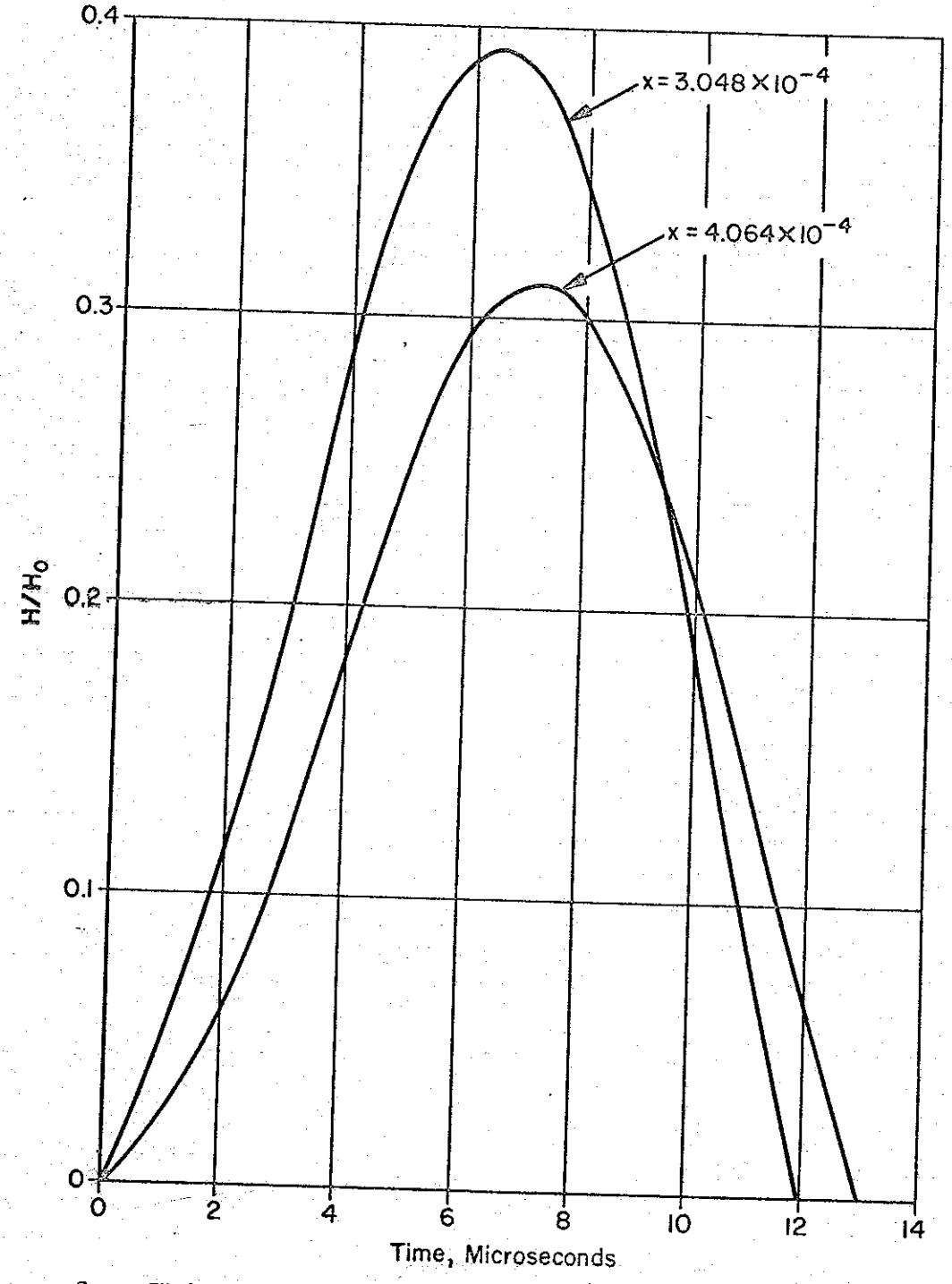

Figure 2. Half-period of oscillation of diffusion field as a function of penetration depth for constant $a = 5 \times 10^4$ sec^{-1} and for constant $\omega = 3.5 \times 10^5$ sec^{-1}.

greater than those of the surface field. However, it is evident from Figure 1 that this is not true in the present instance. For any given penetration depth x, there exists during each half-cycle a well-defined time-interval over which the diffusion field is greater than the corresponding field at the surface. This is a direct consequence of the broadening of the half-period with increasing penetration distance. The spatial profile of the diffusion field at given instants of time is shown in Figure 3. At early times, the field falls off sharply with penetration distance, whereas at six microseconds, the variation with distance is nearly linear. After ten microseconds, the surface field is nearly zero, and the field inside the conductor is greater than the field at the surface.

The complete behavior of the diffusion field cannot be ascertained until the time variation of the field with respect to both the damping rate, a, and the angular frequency, ω, respectively, is determined.

Values of the damping rate and the angular frequency have been chosen to correspond to physically real situations. Values of ω were selected in the range 3 to 4 x 10^5 sec^{-1}, which corresponds to periods of approximately 15 to 20 microseconds. The ratio ω/a usually varies from a low of 3 to a high of 15 for most capacitor banks, thus dictating choices for the damping rate in the range 3 to 10 x 10^4 sec^{-1}.

The time variation of the diffusion field with damping rate is shown in Figures 4, 5, and 6 and in Tables 2, 3, and 4 for constant $x = 3.048 \times 10^{-4}$ meter and constant $\omega = 4.0 \times 10^5$ sec^{-1}, 3.5×10^5 sec^{-1}, and 3.0×10^5 sec^{-1}, respectively. Note that in each instance the field generally decreases with increased damping, as expected, since the surface field, $H_s = H_o e^{-at} \sin \omega t$, also exhibits such behavior. The rise time to peak also decreases with increasing a, which again corresponds to the behavior of the surface field whose time to peak is

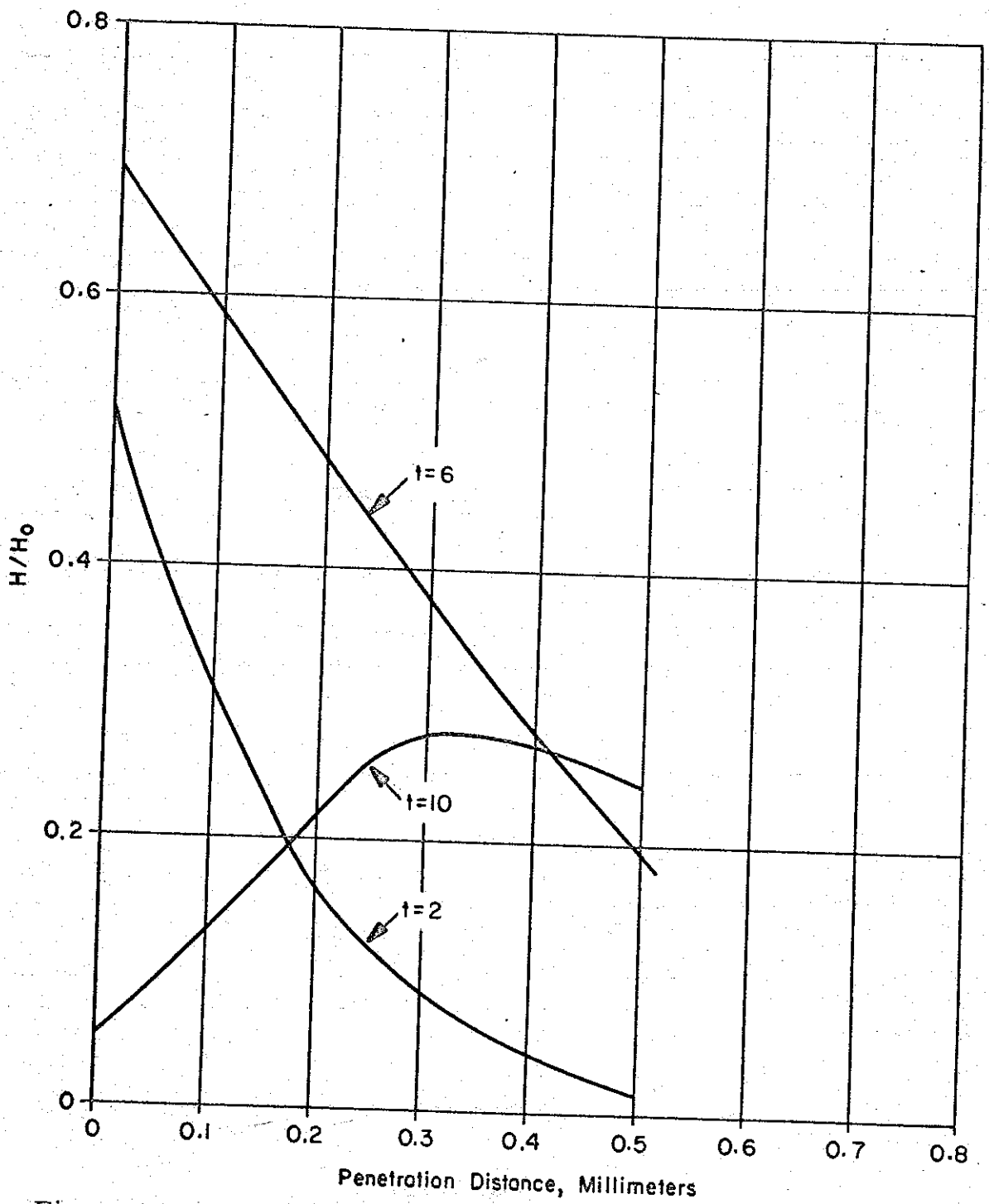

Figure 3. Spatial variation of diffusion field as a function of time for constant $a = 5.4 \times 10^4$ sec^{-1} and for constant $\omega = 3.05 \times 10^5$ sec^{-1}.

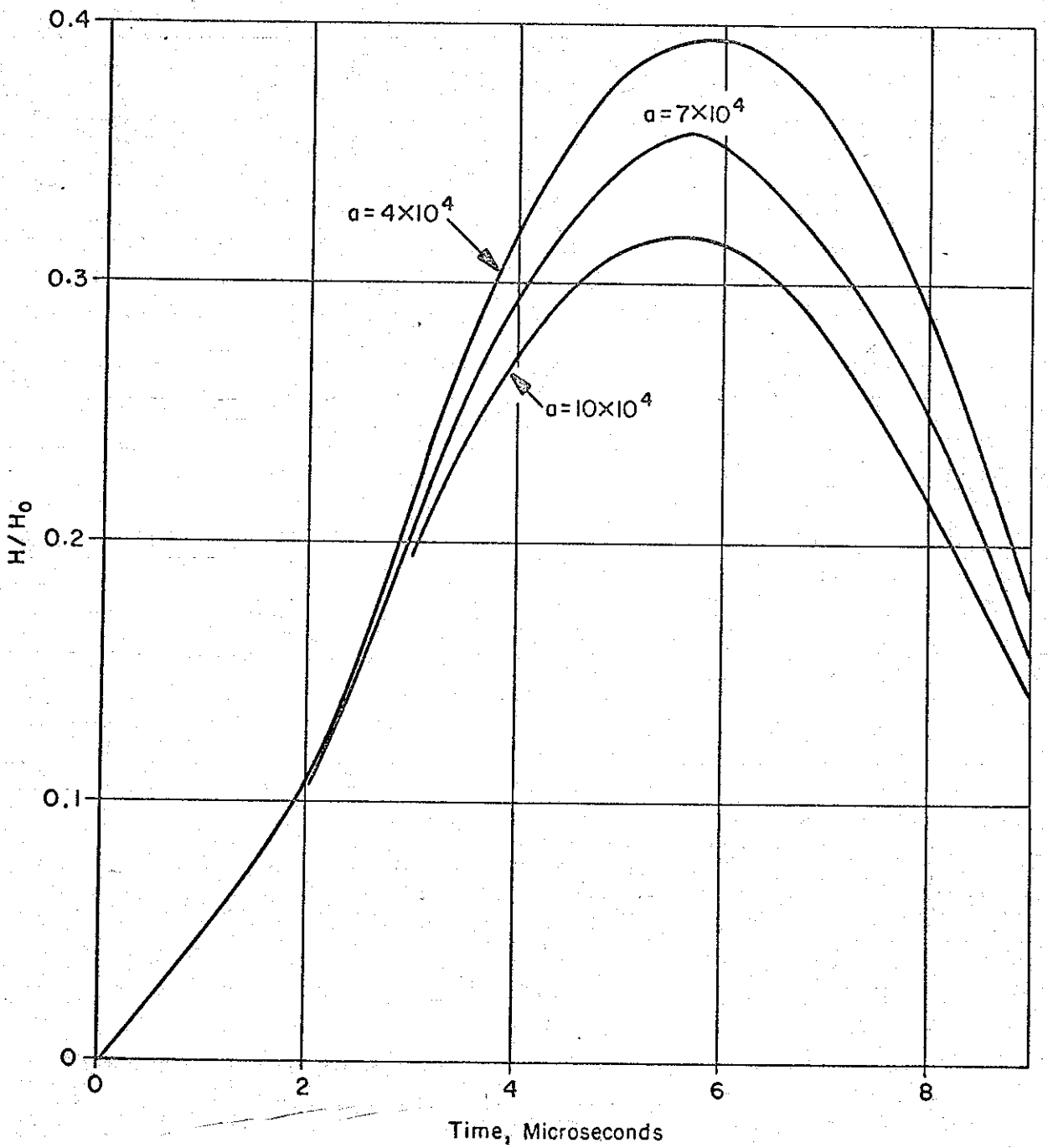

Figure 4. Time variation of diffusion field as a function of the damping rate, a, for constant $\omega = 4.0 \times 10^{5}$ sec^{-1} and for constant $x = 3.048 \times 10^{-4}$ m.

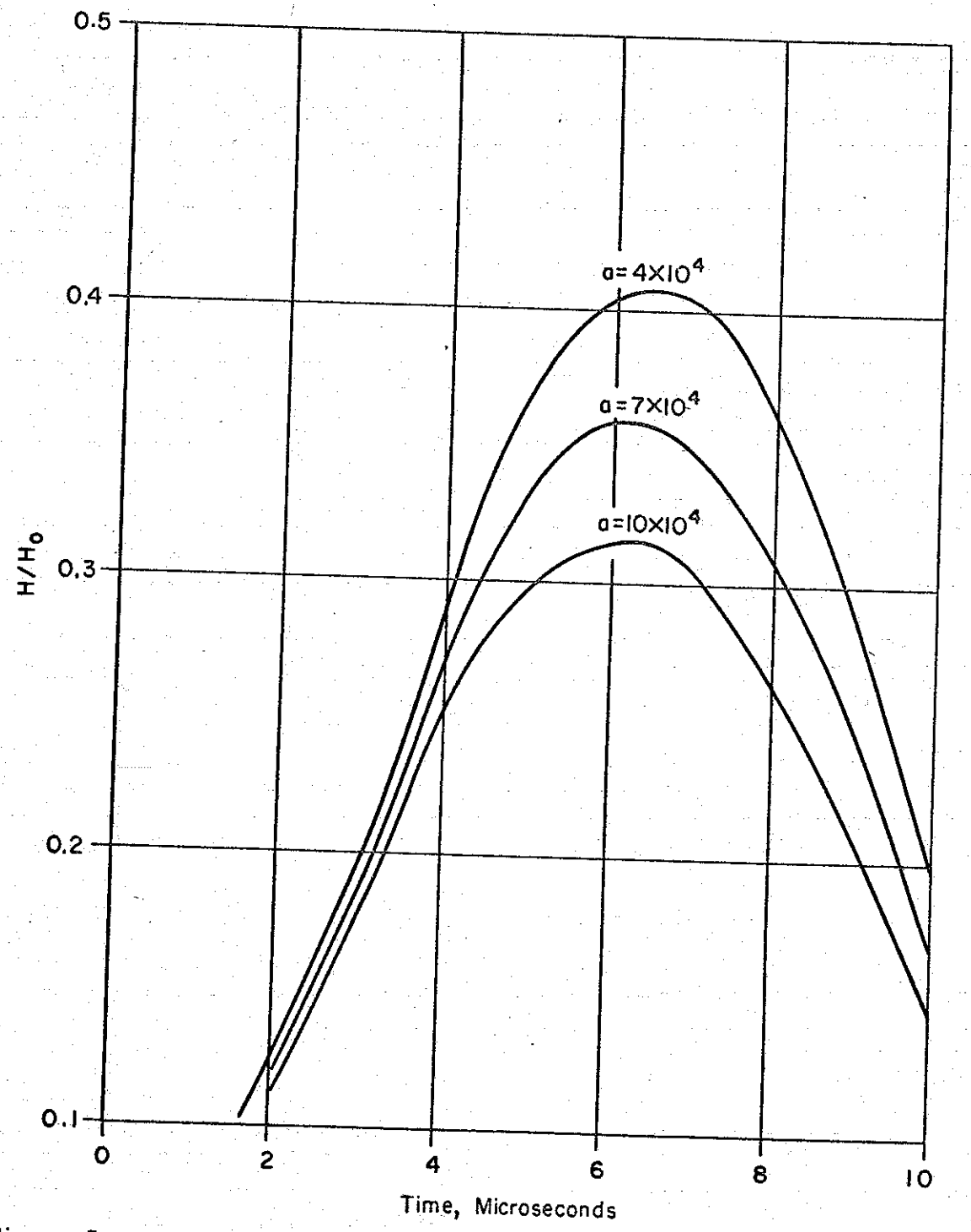

Figure 5. Time variation of diffusion field as a function of the damping rate for constant $\omega = 3.5 \times 10^{5}$ sec^{-1} and for constant $x = 3.048 \times 10^{-4}$ m.

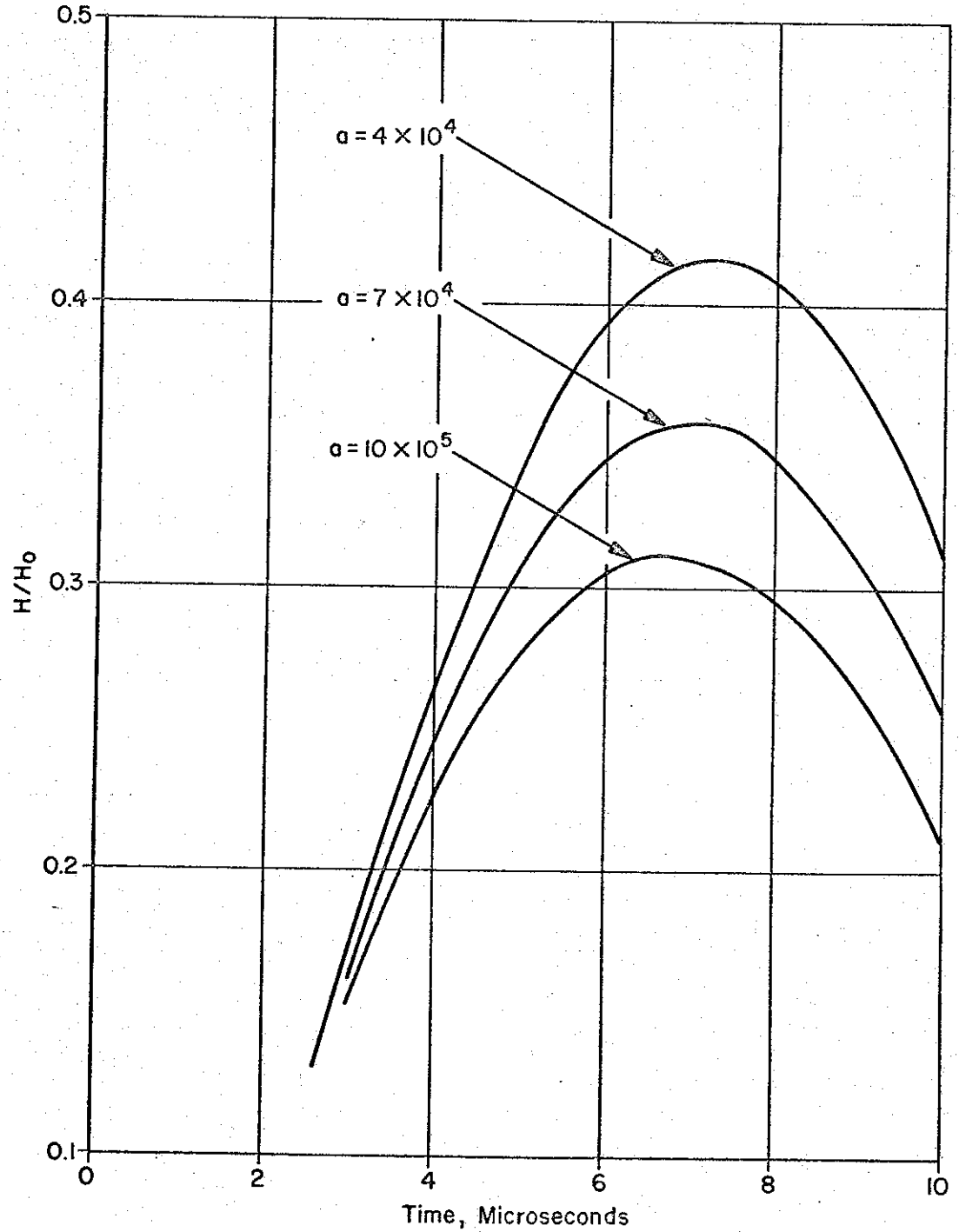

Figure 6. Time variation of diffusion field as a function of the damping rate for constant $\omega = 3.0 \times 10^{5}$ sec^{-1} and for constant $x = 3.048 \times 10^{-4}$ m.

TABLE 2. TIME VARIATION OF H/H_o AS A FUNCTION OF THE DAMPING RATE FOR CONSTANT $\omega = 4.0 \times 10^5$ sec^{-1} AND FOR CONSTANT $x = 3.048 \times 10^{-4}$ m

a	Time, Microseconds							
	2	3	4	5	6	7	8	9
3×10^4	0.109	0.223	0.328	0.395	0.413	0.380	0.302	0.191
4×10^4	0.108	0.218	0.319	0.382	0.396	0.363	0.287	0.182
5×10^4	0.107	0.214	0.310	0.370	0.381	0.347	0.274	0.174
6×10^4	0.106	0.210	0.301	0.357	0.366	0.332	0.262	0.166
7×10^4	0.105	0.207	0.294	0.345	0.352	0.317	0.250	0.159
8×10^4	0.104	0.202	0.287	0.334	0.339	0.303	0.238	0.153
9×10^4	0.103	0.198	0.280	0.323	0.326	0.291	0.227	0.147
10×10^4	0.102	0.194	0.273	0.313	0.314	0.280	0.216	0.141

TABLE 3. TIME VARIATION OF H/H_o AS A FUNCTION OF THE DAMPING RATE FOR CONSTANT $\omega = 3.5 \times 10^5$ sec^{-1} AND FOR CONSTANT $x = 3.048 \times 10^{-4}$ m

a	Time, Microseconds							
	3	4	5	6	7	8	9	10
3×10^4	0.199	0.303	0.380	0.422	0.422	0.382	0.307	0.206
4×10^4	0.195	0.294	0.367	0.404	0.403	0.362	0.289	0.196
5×10^4	0.192	0.286	0.355	0.388	0.385	0.344	0.274	0.187
6×10^4	0.188	0.278	0.343	0.373	0.367	0.327	0.260	0.177
7×10^4	0.185	0.271	0.331	0.358	0.349	0.311	0.246	0.168
8×10^4	0.182	0.264	0.320	0.343	0.333	0.295	0.233	0.160
9×10^4	0.179	0.257	0.309	0.329	0.319	0.279	0.221	0.152
10×10^4	0.176	0.251	0.298	0.315	0.305	0.264	0.209	0.145

TABLE 4. TIME VARIATION OF H/H_o AS A FUNCTION OF THE DAMPING RATE FOR CONSTANT $\omega = 3.0 \times 10^5$ sec^{-1} AND FOR CONSTANT $x = 3.048 \times 10^{-4}$ m

a	Time, Microseconds							
	3	4	5	6	7	8	9	10
3×10^4	0.178	0.272	0.352	0.408	0.435	0.434	0.398	0.336
4×10^4	0.172	0.264	0.339	0.392	0.415	0.409	0.374	0.313
5×10^4	0.168	0.257	0.328	0.375	0.395	0.386	0.352	0.294
6×10^4	0.165	0.251	0.317	0.360	0.376	0.366	0.331	0.276
7×10^4	0.162	0.245	0.307	0.345	0.358	0.347	0.311	0.259
8×10^4	0.159	0.238	0.296	0.331	0.340	0.328	0.294	0.243
9×10^4	0.156	0.232	0.287	0.318	0.325	0.311	0.277	0.229
10×10^4	0.154	0.225	0.277	0.305	0.310	0.295	0.262	0.213

$$t_{max} = \frac{1}{\omega} \tan^{-1} \frac{\omega}{a} \quad . \qquad (34)$$

Although the period of the surface field is not dependent on the damping rate, Figure 7 clearly shows that the half-period of the diffusion field increases with increasing a. This variation is unusual because the rise time to peak decreases with increasing a.

It is also of interest to determine the fraction of the surface field that diffuses to a given penetration depth during the first quarter-cycle. The plots in Figures 4, 5, and 6 do not reveal the answer to this query because the surface field also varies as a function of the damping rate. Accordingly, the difference $\Delta H = H_s - H(x, t)$ has been plotted in Figure 8 for constant values of ω and x, and the ratio $h = H(x, t)/H_s$ has been plotted in Figure 9. One can readily observe from these two plots that the percentage diffusion increases with the damping rate. Values of ΔH and h are listed as functions of a and t in Tables 5 and 6, respectively.

One must still investigate the dependence of H(x, t) on the angular frequency, ω. One expects, as shown in Figure 10, that both the rise time to peak and the half-period will decrease with increasing frequency, since the surface field exhibits such properties. However, for the surface field, the peak value of the field increases with increasing frequency as shown in Figure 11. The converse is true regarding the diffusion field as revealed in Figure 10. This implies that the percentage diffusion increases markedly as the ringing frequency, ω, is lowered.

The salient features of the above analysis are summarized below.

A. All other parameters being held constant, the rise time to peak of the diffusion field

1. increases with increasing penetration depth,

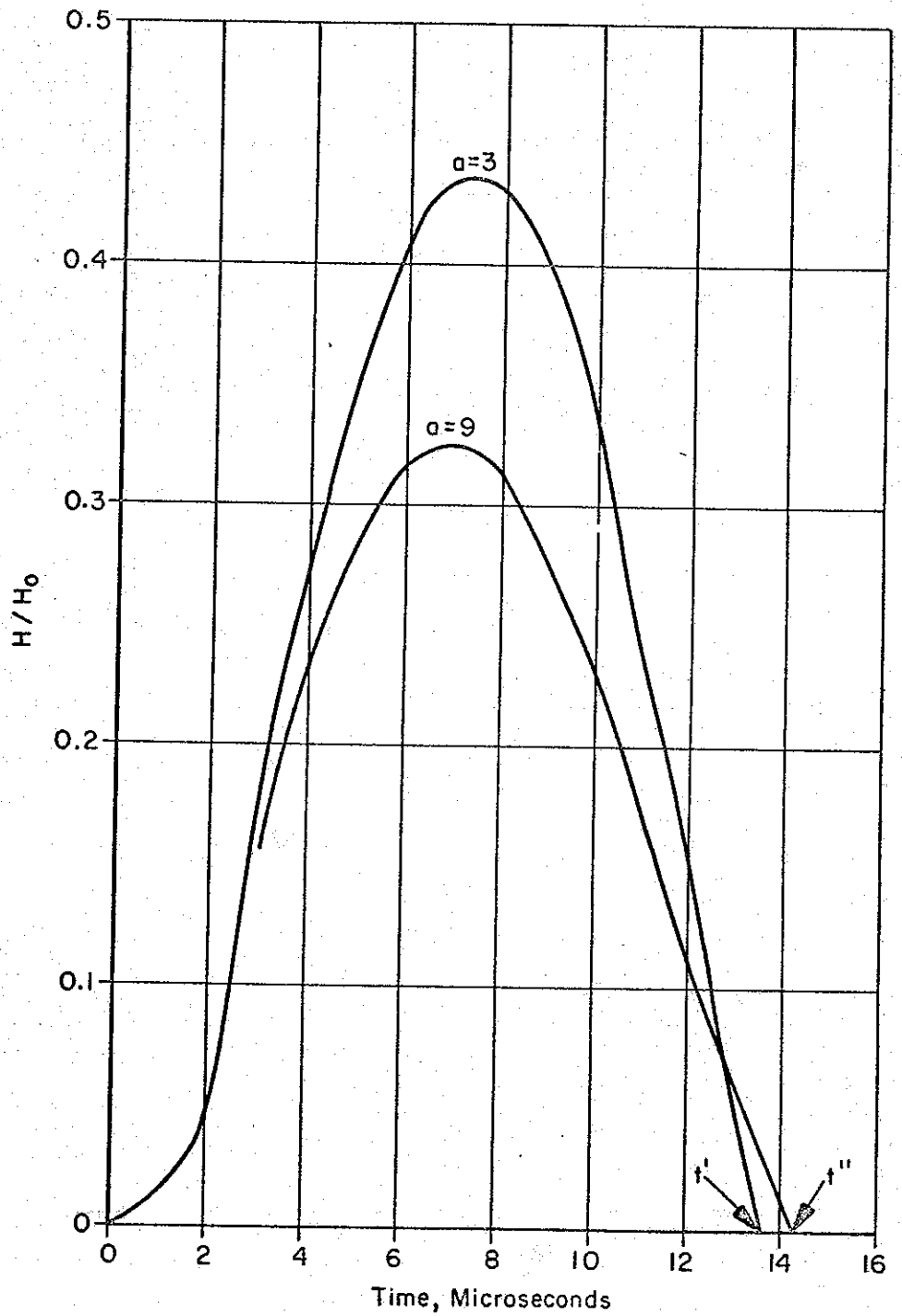

Figure 7. Variation of half-period of diffusion field with the damping rate for constant $\omega = 3.0 \times 10^{5}$ sec^{-1} and for constant $x = 3.048 \times 10^{-4}$ m.

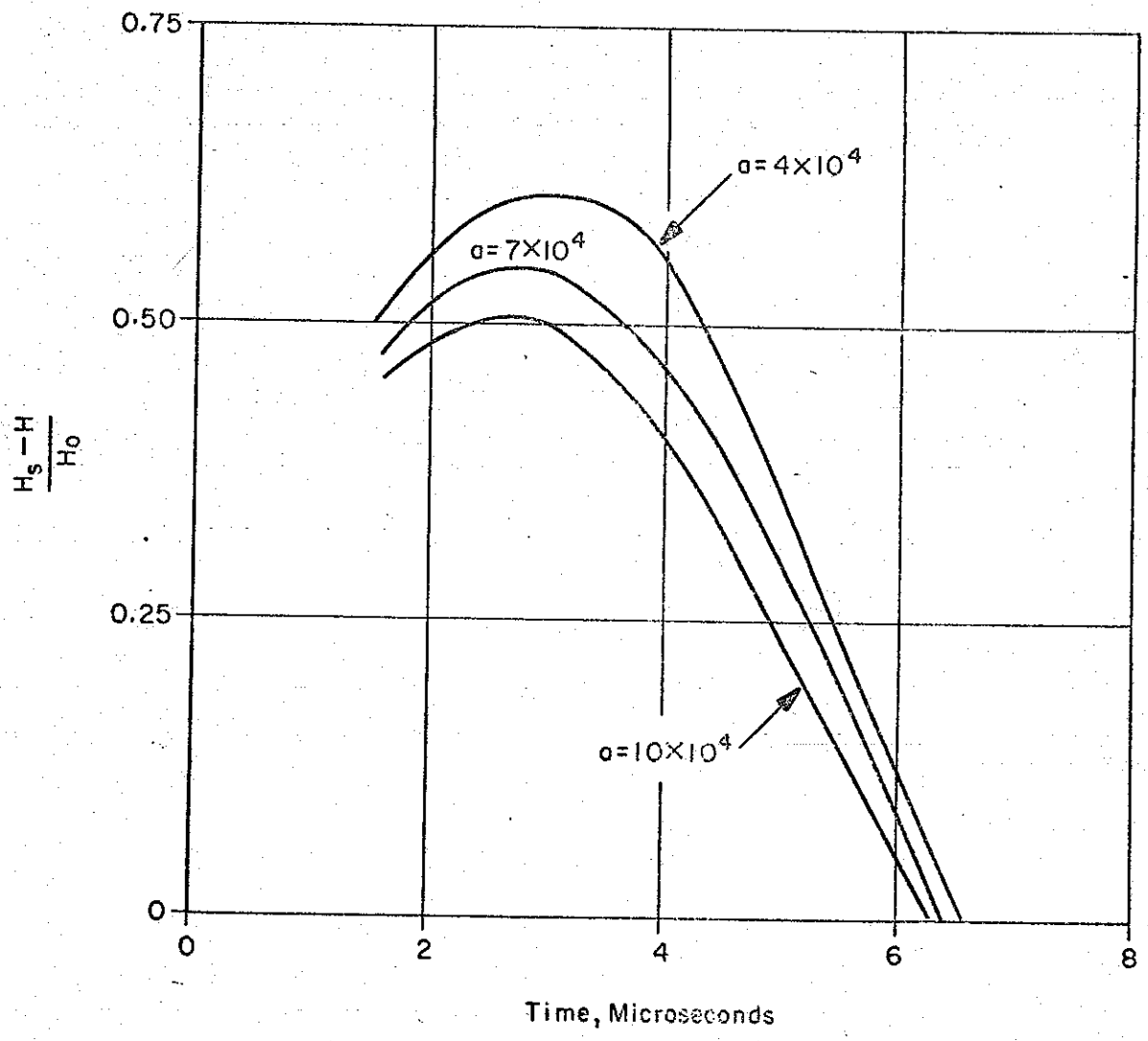

Figure 8. Difference between surface and diffusion fields; time variation as a function of the damping rate for constant $\omega = 4 \times 10^5$ sec^{-1} and for constant $x = 3.048 \times 10^{-4}$ m.

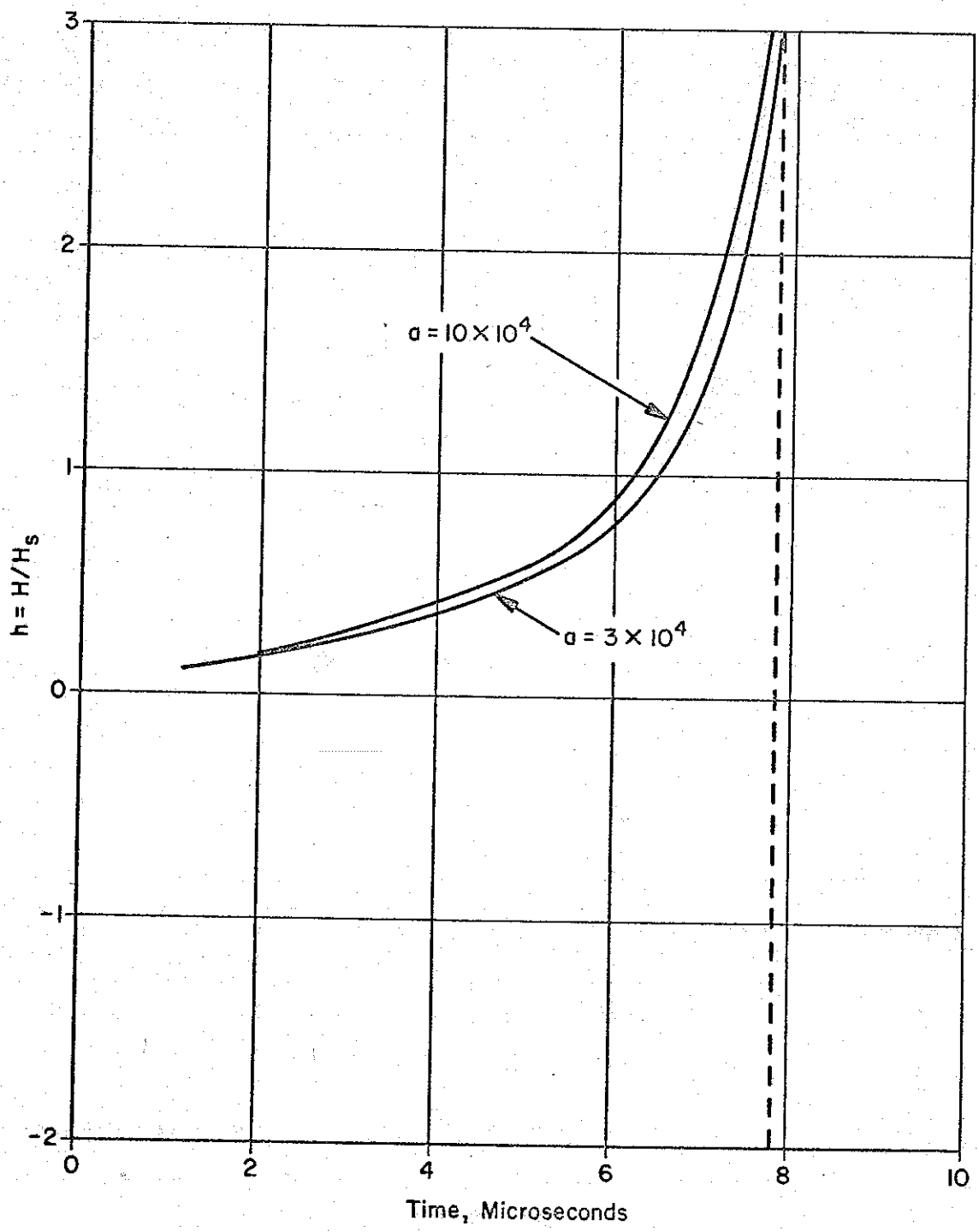

Figure 9. Ratio of diffusion field to surface field; time variation as a function of the damping rate for constant $\omega = 4.0 \times 10^{5}$ sec^{-1} and for constant $x = 3.048 \times 10^{-4}$ m.

TABLE 5. TIME VARIATION OF $\Delta H = \frac{H_s - H}{H_o}$ AS A FUNCTION OF THE DAMPING RATE FOR CONSTANT $\omega = 4.0 \times 10^5$ sec^{-1} AND FOR CONSTANT $x = 3.048 \times 10^{-4}$ m

a	Time, Microseconds							
	2	3	4	5	6	7	8	9
$3x10^4$	0.567	0.629	0.559	0.388	0.150	-0.110	-0.348	-0.528
$4x10^4$	0.554	0.608	0.532	0.361	0.134	-0.111	-0.329	-0.488
$5x10^4$	0.542	0.588	0.508	0.338	0.119	-0.112	-0.313	-0.455
$6x10^4$	0.530	0.568	0.495	0.317	0.105	-0.112	-0.298	-0.424
$7x10^4$	0.519	0.548	0.462	0.296	0.091	-0.113	-0.283	-0.394
$8x10^4$	0.507	0.529	0.439	0.274	0.078	-0.113	-0.269	-0.367
$9x10^4$	0.496	0.513	0.417	0.253	0.007	-0.113	-0.255	-0.343
$10x10^4$	0.485	0.498	0.396	0.232	0.056	-0.113	-0.242	-0.320

TABLE 6. TIME VARIATION OF $h = H/H_s$ AS A FUNCTION OF THE DAMPING RATE FOR CONSTANT $\omega = 4.0 \times 10^5$ sec^{-1} AND FOR CONSTANT $x = 3.048 \times 10^{-4}$ m

a	Time, Microseconds							
	2	3	4	5	6	7	8	9
$3x10^4$	0.161	0.262	0.370	0.504	0.734	1.407	-6.571	-0.567
$4x10^4$	0.163	0.264	0.374	0.513	0.747	1.441	-6.792	-0.592
$5x10^4$	0.165	0.267	0.379	0.523	0.762	1.477	-7.030	-0.619
$6x10^4$	0.167	0.270	0.384	0.531	0.778	1.514	-7.306	-0.647
$7x10^4$	0.168	0.273	0.389	0.540	0.795	1.554	-7.582	-0.677
$8x10^4$	0.170	0.275	0.395	0.550	0.812	1.594	-7.860	-0.711
$9x10^4$	0.172	0.278	0.402	0.561	0.830	1.635	-8.154	-0.750
$10x10^5$	0.174	0.280	0.409	0.571	0.848	1.677	-8.452	-0.790

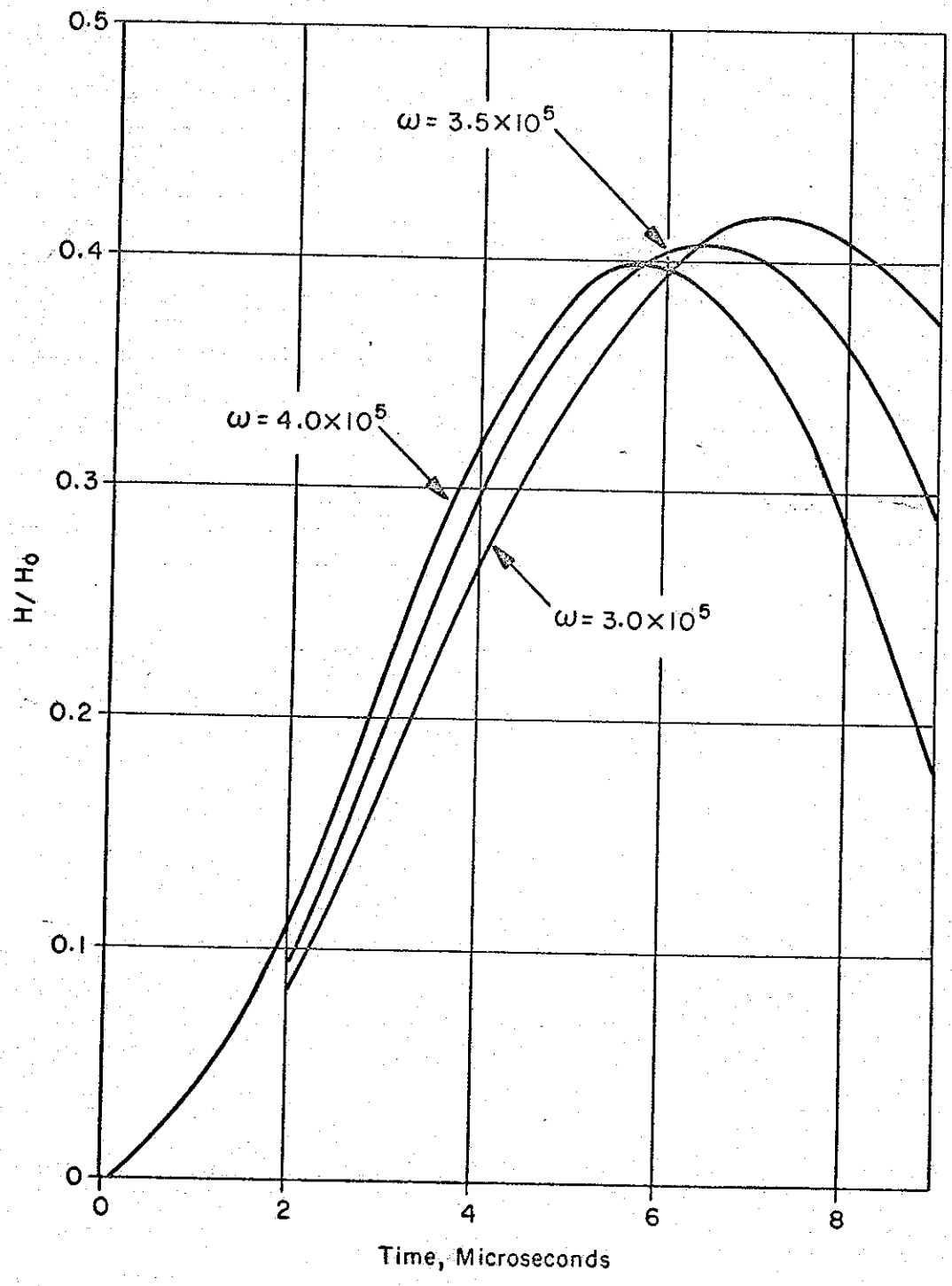

Figure 10. Time variation of diffusion field as a function of frequency for constant a = 4×10^{4} sec^{-1} and for constant x = 3.048×10^{-4} m.

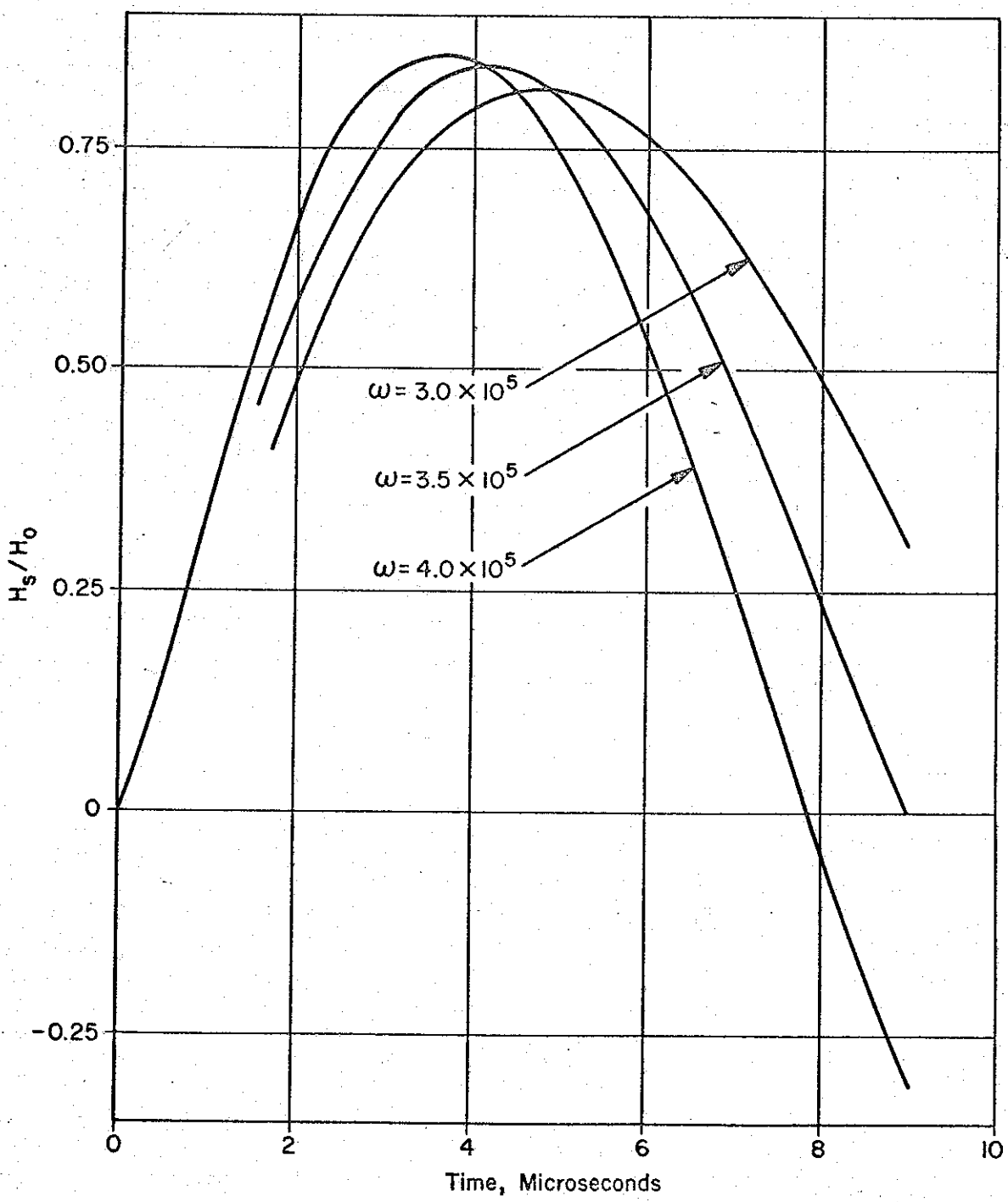

Figure 11. Time variation of surface field $e^{-at} \sin \omega t$ as a function of frequency for constant $a = 4 \times 10^4$ sec^{-1}.

2. increases with decreasing damping rate, and
3. increases with decreasing frequency.

B. All other parameters being held constant, the length of the half-period of oscillation

1. increases with increasing penetration depth,
2. increases with increasing damping rate, and
3. increases with decreasing frequency.

C. All other parameters being held constant, the percentage diffusion

1. increases with decreasing penetration depth,
2. increases with increasing damping rate, and
3. decreases with increasing frequency.

1. Mathews, J. and R. L. Walker; Mathematical Methods of Physics; W. A. Benjamin, Inc., New York City; 1964; pp. 228-230.

2. Kidder, R. E.; "Non-Linear Diffusion of Strong Magnetic Fields into a Conducting Half Space"; UCRL-5467; Lawrence Radiation Laboratory, University of California, Livermore, California; January 1959; pp. 3-6.

3. Handbook of Chemistry and Physics, 42nd edition; Chemical Rubber Publishing Co., Cleveland, Ohio; 1960; pp. 293-299.

4. Carslaw, H. S. and J. C. Jaeger; Conduction of Heat in Solids, 2nd edition; Clarendon, Press, Oxford, England; 1959; pp. 494-495.

5. Gautschi, W.; "Error Function and Fresnel Integrals" in Handbook of Mathematical Functions; Applied Mathematics Series 55, National Bureau of Standards, Washington, D. C.; March 1965; Chapter 7.